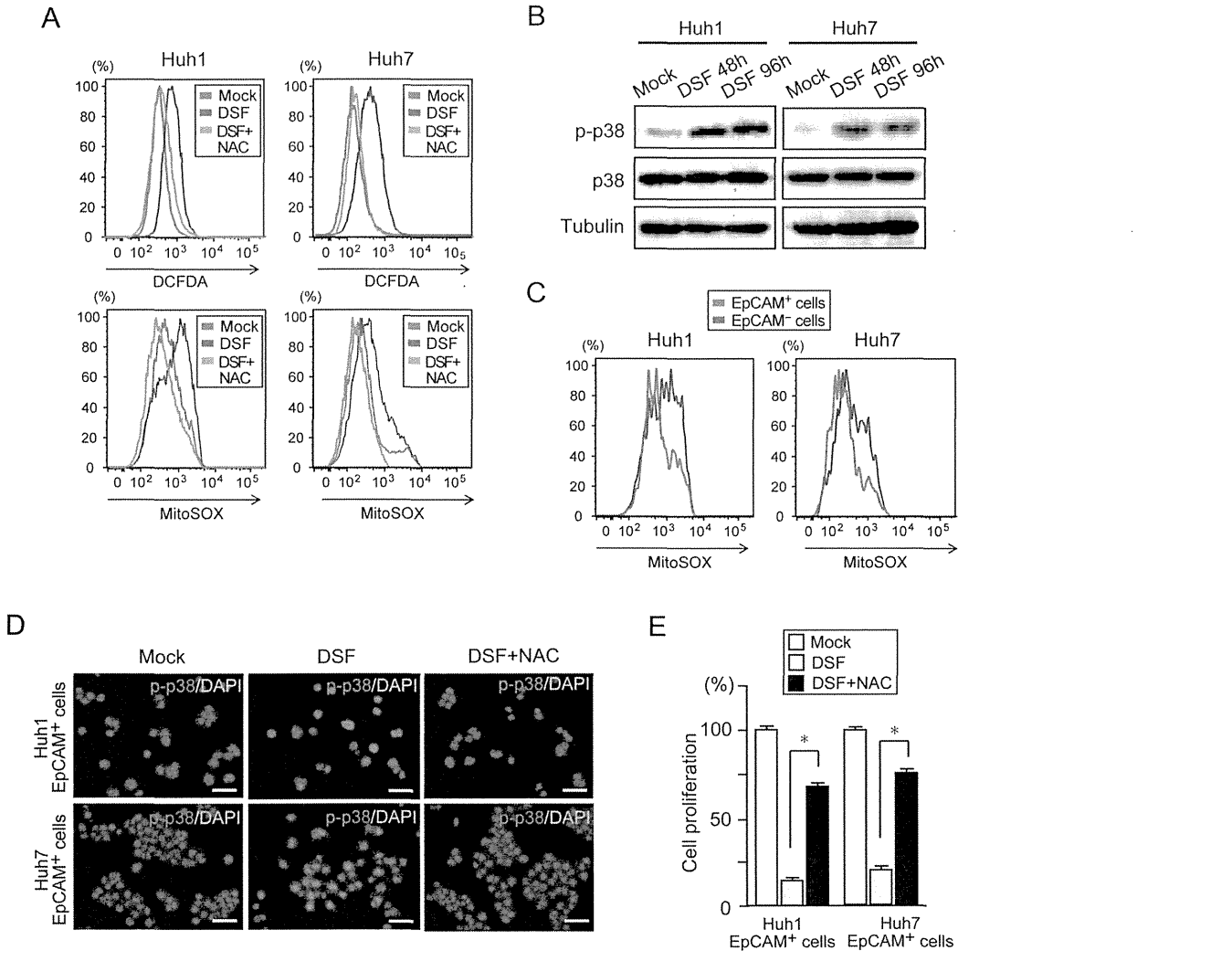

Figure 3. Activation of the ROS-p38 MAPK pathway in tumor-initiating EpCAM$^+$ cells treated with DSF. (A) Flow cytometric analysis of ROS levels. Intracellular ROS concentrations were measured by DCFDA and MitoSOX staining. (B) Cells treated with DSF for 48 or 96 hours were subjected to Western blot analysis using phospho-p38 (p-p38), p38, and anti-tubulin (loading control) antibodies. (C) Flow cytometric analysis of ROS levels in view of EpCAM expression. Intracellular ROS concentrations were measured by MitoSOX staining. (D) Fluorescence images of EpCAM$^+$ HCC cells. The expression of p-p38 (red) was merged with nuclear DAPI staining (blue). Scale bar = 100 μm. (E) Proliferation of EpCAM$^+$ HCC cells at 96 hours in culture. The percentages of cells are shown. *Statistically significant ($p<0.05$).
doi:10.1371/journal.pone.0084807.g003

blot analysis of these cells showed that both shRNAs against *GPC3* (sh-*GPC3*-1 and sh-*GPC3*-2) markedly repressed GPC3 expression, although sh-*GPC3*-1 was more effective than sh-*GPC3*-2 (Figure 6C). *GPC3*-knockdown suppressed cell growth and induced apoptosis relative to sh-*Luc* (Figure S7C and S7D). Similarly, *GPC3*-knockdown markedly impaired primary sphere formation by EpCAM$^+$ cells and EpCAM$^-$ cells and more severely impaired secondary sphere formation (Figure 6D-F). Immunocytochemical analyses of the large spheres showed a decrease in the number of cells expressing AFP or EpCAM (Figure S7E and S7F). In contrast, the stable overexpression of *GPC3* promoted cell growth and sphere formation of tumor-initiating HCC cells (Figure S8). Together, these results indicate that *GPC3*-knockdown suppresses tumorigenicity of HCC cells by directly affecting the cell growth and the self-renewal of TIC.

Discussion

High levels of ALDH activity are characteristic of normal stem cells in a variety of organs. The human ALDH superfamily consists of 19 putatively functional genes [22]. ALDH1 is a major isoform in mammalian tissues and functions as a stem cell marker in liver and mammary stem cells [23,24]. Recent reports have indicated ALDH1 to be a useful marker for the enrichment of TICs from various cell lines and primary tumors. It has been shown that a high level of ALDH1 expression correlates with malignant phenotypes and an unfavorable prognosis in a range of cancers [24].

In this study, we first showed that DSF inhibited the proliferation and sphere-forming ability of HCC cells in a dose-dependent manner. In addition, DSF suppressed tumor growth in xenograft transplant experiments using NOD/SCID mice. Our flow cytometric analysis showed that the DSF treatment caused a significant decrease in the number of tumor-initiating HCC cells

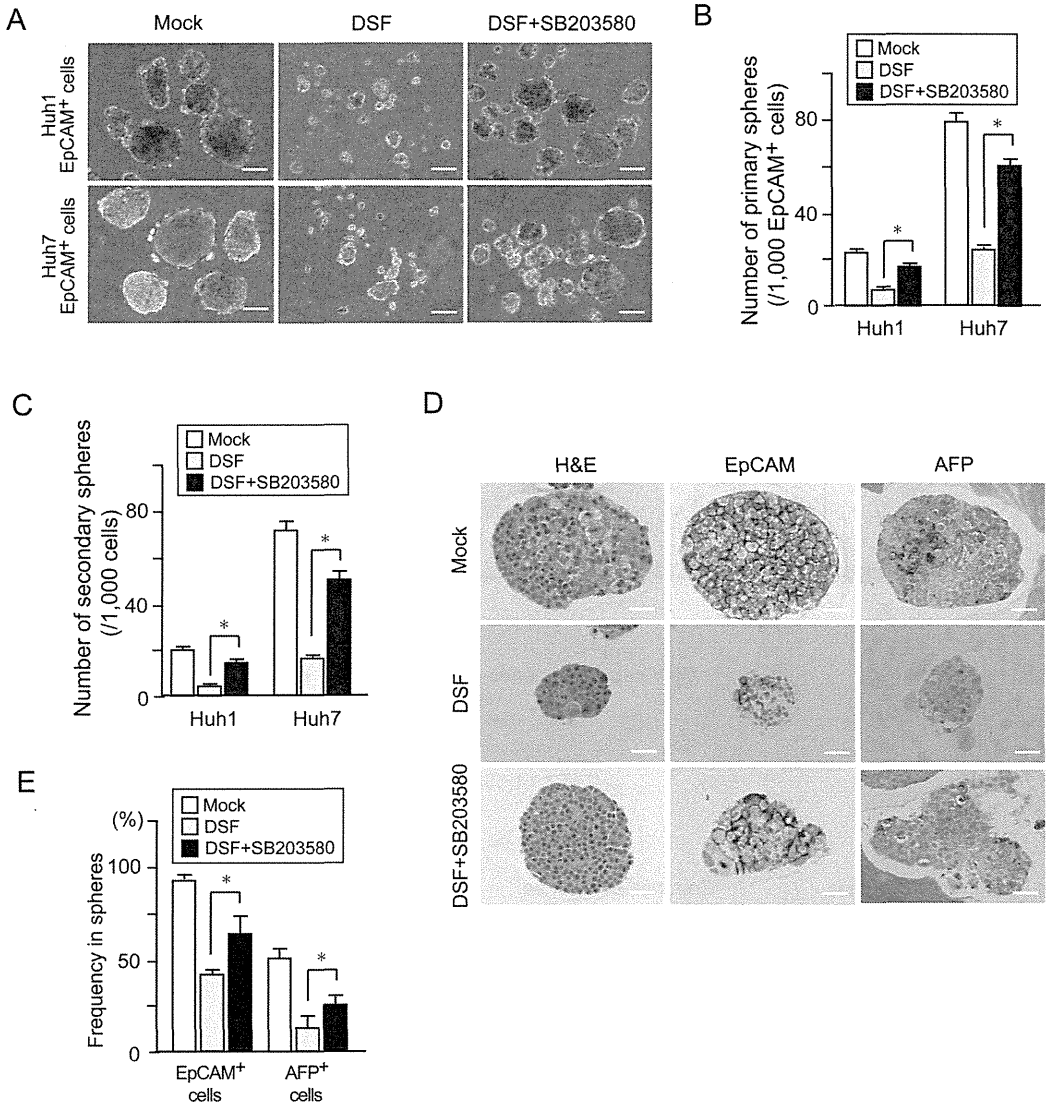

Figure 4. Sphere formation assays and immunocytochemical analyses in tumor-initiating EpCAM$^+$ cells treated with a p38 inhibitor (SB203580). (A) Bright-field images of non-adherent spheres on day 14 of culture. Scale bar = 100 μm. (B) Number of large spheres derived from 1,000 EpCAM$^+$ tumor cells on day 14 of culture. *Statistically significant ($p<0.05$). (C) Number of secondary spheres 14 days after replating. *Statistically significant ($p<0.05$). (D) H&E staining and immunocytochemical analysis of EpCAM and AFP in spheres derived from EpCAM$^+$ cells. (E) Quantification of the percentage of EpCAM$^+$ cells or AFP$^+$ cells. *Statistically significant ($p<0.05$).
doi:10.1371/journal.pone.0084807.g004

expressing surface markers such as CD13, CD133, and EpCAM. Knockdown of *ALDH1* and *ALDH2* in HCC cells had no effect on cell proliferation and sphere-forming ability in the culture. Our findings suggest that DSF exerts its anti-HCC function in an ALDH-independent fashion.

HSCs have been shown to tightly control intracellular ROS levels to maintain long-term self-renewal and survival [25]. Conversely, activation of p38 MAPK upon an elevation in ROS levels resulted in the exhaustion of HSCs [26]. Similarly, TICs in a wide range of tumors exhibited lower concentrations of ROS than corresponding non-TICs. In addition, lower ROS levels in TICs were shown to be closely associated with both chemo-sensitivity and radio-sensitivity [15]. In the present study, we confirmed that EpCAM$^+$ HCC cells contained lower ROS levels than EpCAM$^-$ cells. Because previous studies reported that DSF activated the ROS-p38 MAPK pathway and thereby suppressed the sphere-forming ability of TICs [6,7], we examined whether exposure to DSF activated the ROS-p38 MAPK pathway in tumor-initiating HCC cells. As expected, the treatment of EpCAM$^+$ HCC cells with NAC canceled p38 activation. Moreover, the SB203580 treatment largely restored the tumorigenicity of EpCAM$^+$ HCC cells. These findings indicate that the ROS-p38 MAPK pathway is directly associated with cell growth and tumor-initiating capability of HCC cells. Low levels of ROS in TICs have been attributable to the activation of the ROS scavenger pathway [27]. The present microarray results showed comparatively high expression levels of ROS scavenger genes such as *GCLM* and *GSS* in purified EpCAM$^+$ HCC cells. However, the DSF treatment caused no marked changes to the ROS scavenger genes. Considering that not only H2DCFDA staining but also MitoSOX staining showed a high ROS level in DSF-treated EpCAM$^+$ HCC cells, DSF might increases mitochondrial ROS production rather than impairs the scavenging of ROS. Further analysis is required to clarify this point.

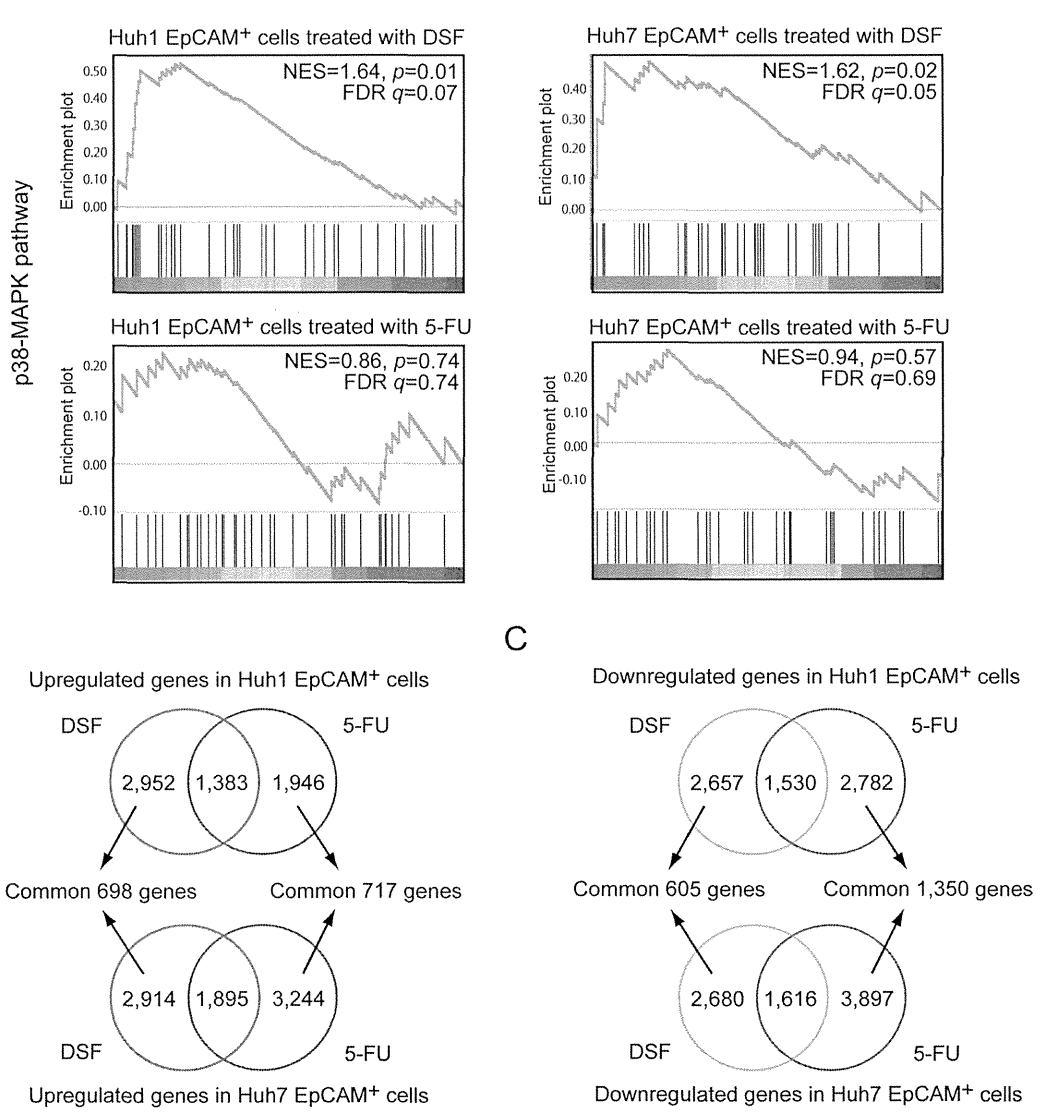

D

Downregulated genes annotated as "liver cancer" in functional analysis

UniGene	Symbol	UniGene	Symbol
Hs.442182	ABCC6	Hs.426485	HPX
Hs.334707	ACY1	Hs.524513	HSD17B6
Hs.530274	ALDOB	Hs.282735	NR1H4
Hs.052968	APOA5	Hs.654800	PNPLA3
Hs.461086	CDH1	Hs.525557	SERPINA1
Hs.84113	CDKN3	Hs.436893	SLC15A1
Hs.647036	CLDN4	Hs.656544	SOAT2
Hs.129798	DGAT2	Hs.71465	SQLE
Hs.304682	CST3	Hs.478265	TNFSF10
Hs.118681	ERBB3	Hs.351815	TPD52
Hs.333303	GJB1	Hs.108049	UACA
Hs.644108	GPC3		

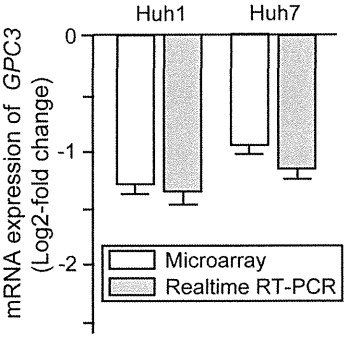

Figure 5. Gene expression profiles of EpCAM$^+$ cells treated with DSF or 5-FU. (A) Gene set enrichment analysis (GSEA) of the p38-MAPK signaling pathway. Both the normalized enrichment score (NES) and false discovery rate (FDR) are shown in each enrichment plot. (B) Common upregulated genes in Huh1 cells (upper panel) and Huh7 cells (lower panel) after DSF or 5-FU treatment are depicted in Venn diagrams. (C) Common downregulated genes in Huh1 cells (upper panel) and Huh7 cells (lower panel) after DSF or 5-FU exposure are depicted in Venn diagrams. (D) A list of

downregulated genes annotated as "liver cancer" in DSF-treated EpCAM$^+$ HCC cells. (E) The expression of *GPC3* in DSF-treated EpCAM$^+$ cells was compared to that in control cells. The data obtained by microarray analyses and quantitative RT-PCR analyses are presented.
doi:10.1371/journal.pone.0084807.g005

Of interest, our microarray analyses revealed that DSF acted in a manner different from 5-FU. The GSEA results support the present biological finfings and implicate the activation of p38 in the anti-TIC activity of DSF. Importantly, the 23 genes in the "liver cancer" category were significantly downregulated after the DSF exposure, but none of them was significantly altered after the 5-FU treatment. One of these genes, GPC3, was frequently overexpressed in HCC and increased GPC3 expression was correlated with a poor prognosis among HCC patients [20,21]. A clinical trial using a GPC3 peptide vaccine in patients with advanced HCC has also been carried out [28]. While GPC3 functions as a marker for normal hepatic stem/progenitor cells [29], the immunostaining analyses showed an association between the expression of EpCAM and GPC3 in both HCC cell lines and

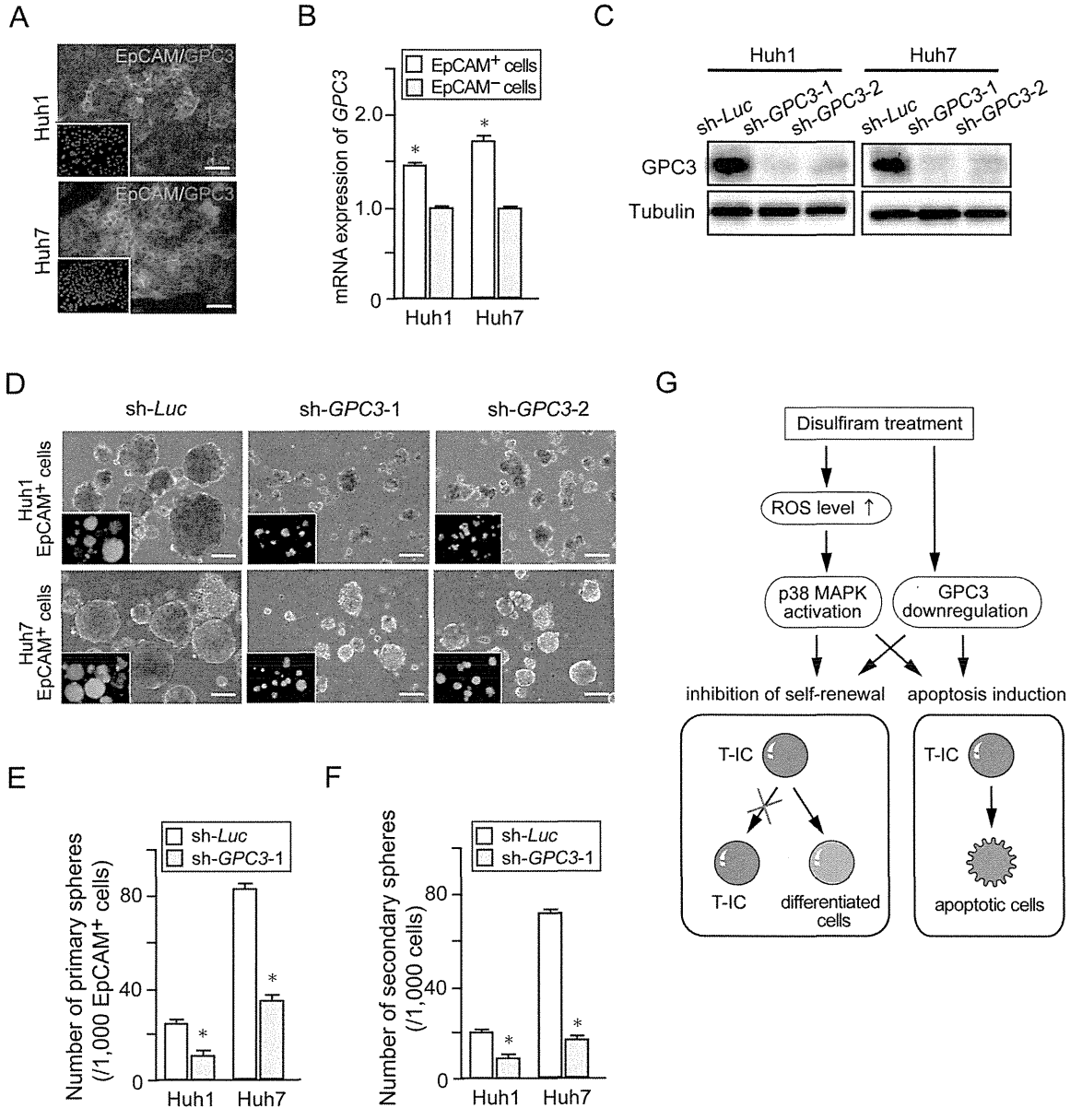

Figure 6. Impact of *GPC3* depletion on sorted EpCAM$^+$ HCC cells. (A) Dual immunostaining was performed to detect the expression of EpCAM (green) and GPC3 (red). Nuclear DAPI staining is shown in the insets. Scale bar = 100 μm. (B) Real-time RT-PCR analysis of GPC3 expression in purified EpCAM$^+$ cells. *Statistically significant ($p<0.05$). (C) Cells transduced with the indicated lentiviruses were subjected to Western blotting using anti-GPC3 and anti-tubulin (loading control) antibodies. (D) Bright–field images of non-adherent spheres on day 14 of culture. Fluorescence images are shown in the insets. Scale bar = 100 μm. (E) Number of large spheres derived from 1,000 EpCAM$^+$ or EpCAM$^-$ cells at day 14 of culture. *Statistically significant ($p<0.05$). (F) Number of secondary spheres 14 days after replating. *Statistically significant ($p<0.05$). (G) A proposed model for the effect of DSF in targeting tumor-initiating HCC cells.
doi:10.1371/journal.pone.0084807.g006

HCC surgical specimens (data not shown) and the higher basal expression of GPC3 in $EpCAM^+$ cells than $EpCAM^-$ cells. Lentiviral knockdown of *GPC3* significantly reduced the sphere-forming ability of $EpCAM^+$ HCC cells. Additionally, replating assays and immunocytochemical analyses of EpCAM and AFP indicated that GPC3 regulated tumor-initiating HCC cells. Although it appears that DSF suppresses the tumorigenicity of tumor-initiating HCC cells in part by downregulating GPC3 expression, further analyses would be of importance to clarify the mechanisms underlying the downregulation of *GPC3* by DSF.

Finally, our findings successfully demonstrated that DSF significantly reduced the number of tumor-initiating HCC cells through apoptosis induction and the conversion to non-TICs. These effects appeared to be attributable to the activation of the ROS-p38 MAPK pathway and gene silencing with GPC3 (Figure 6G). Further analyses of the genes listed here are necessary to determine the effects of DSF. Recent reports showed that TICs of brain tumors reside in vascular niches in which endothelial cells maintain the TICs in an undifferentiated state [30]. Bevacizumab, a vascular endothelial growth factor (VEGF)-specific inhibitor, causes a drastic decrease in the number of TICs in vascular niches by inhibiting the self-renewal of TICs [31]. Although the niche for TICs in HCC remains to be elucidated, combination therapy using DSF and the anti-angiogenic multi-kinase inhibitor sorafenib might be effective in the eradication of tumor-initiating HCC cells.

Materials and Methods

Ethics statement

All experiments using the mice were performed in accordance with our institutional guidelines for the use of laboratory animals and approved by the review board for animal experiments of Chiba University (approval ID: 22–187).

Mice

Nonobese diabetic/severe combined immunodeficiency (NOD/SCID) mice (Sankyo-Lab Service, Tsukuba, Japan) were bred and maintained in accordance with our institutional guidelines for the use of laboratory animals.

Cell culture and reagents

The HCC cell lines were obtained from the Health Science Research Resources Bank (HSRRB, Osaka, Japan). DSF was kindly provided by Mitsubishi Tanabe Pharma Corporation. Cells were treated with DSF/$CuCl_2$ (0.1 or 1 μM) or 5-FU (1 μM; Sigma-Aldrich, St Louis, MO). Cells were treated with MG132 (10 μM, Cayman Chemical, Ann Arbor, MI), *N*-Acetyl-L-cysteine (NAC) (10 μM, Sigma), and SB203860 (10 mM, Sigma).

Non-adherent sphere culture

For the sphere formation assay of Huh1, Huh6 and Huh7 cells, 1,000 cells were plated onto ultra-low attachment 6-well plates (Corning, Corning, NY). For the assay of PLC/PRF/5 cells, 500 cells were plated onto NanoCulture 24-well plates (Scivax, Kawasaki, Japan). The number of spheres (>100 μm in diameter) was counted on day 14 of culture. For the secondary sphere formation, a single cell suspension derived from primary colonies was obtained using a Neurocult chemical dissociation kit (StemCell Technologies, Vancouver, BC). Paraffin-embedded sections of the spheres were subjected to hematoxylin & eosin (H&E) staining and immunohistochemical staining with anti-EpCAM (Cell Signaling Technology, Beverly, MA) and anti-AFP (Dako Cytomation, Carpinteria, CA) antibodies.

Cell sorting and analysis

Single-cell suspensions were stained with allophycocyanin (APC)-conjugated anti-EpCAM antibody and anti-CD13 antibody (Biolegend, San Diego, CA) or APC-conjugated anti-CD133/1 antibody (Miltenyi Biotec, Auburn, CA). After the incubation, 1 μg/ml of propidium iodide was added to eliminate dead cells. Flow cytometirc cell sorting and analyses were performed using FACSAria or FACSCanto (BD Biosciences, San Jose, CA). Intracellular ROS levels were determined by flow cytometry using H2DCFDA (Sigma) and MitoSOX (Molecular Probes, Eugene, OR) staining.

Xenograft transplantation using NOD/SCID mice

A total of 2×10^6 Huh1 and Huh7 cells were suspended in DMEM and Matrigel (BD) (1:1). The cells were implanted into the subcutaneous space of the backs of NOD/SCID mice. DSF (10 or 50 mg/Kg) was administered intraperitoneally every other day.

Western blotting

DSF-treated HCC cells were subjected to Western blot analysis using anti-p38 (Santa Cruz Biotechnology, Santa Cruz, CA), anti-phospho-p38 (Cell Signaling Technology), and anti-tubulin (Oncogene Science, Cambridge, MA) antibodies. *ALDH2*-knockdown cells and *ALDH1*-and *ALDH2*-double knockdown cells were subjected to Western blotting using anti-ALDH1 (BD Biosciences) and anti-ALDH2 (Abcam, Cambridge, MA) antibodies. *GPC3*-knockdown cells selected by cell sorting for enhanced green fluorescent protein (EGFP) expression were also subjected to Western blot analysis using anti-GPC3 antibody (Santa Cruz Biotechnology).

Lentiviral production and transduction

A lentiviral vector carrying ERP (CS-H1-shRNA-RfA-ERP) expressing shRNAs against *ALDH2* (target sequence: sh-*ALDH2*-1, 5′-GCCCACTGTGTTTGGAGATGT-3′; sh-*ALDH2*-2, 5′-GCTGTCTTCACAAAGGATTTG-3′) was constructed for the double knockdown of *ALDH1* and *ALDH2*. Lentiviral vectors (CS-H1-shRNA-EF-1a-EGFP) expressing shRNAs against murine GPC3 (target sequence: sh-*GPC3*-1, 5′-GGCTCTGAATCTTG-GAATTGA-3′; sh-*GPC3*-2, 5′-GGGACTGATGATGGT-TAAACC-3′) were also constructed. Recombinant lentiviruses were produced as described elsewhere [32].

Generation of stable GPC3-expressing cells

Human GPC3 cDNA was cloned into a site upstream of IRES-neomycin in the pLP-IRESneo vector (Clontech, Palo. Alto, CA). Stable transfection into Huh1 cells with G418 selection was performed.

Reverse transcription-polymerase chain reaction (RT-PCR)

Quantitative RT-PCR was performed with an ABI PRISM 7300 Sequence Detection System (Applied Biosystems) using the Universal Probe Library System (Roche Diagnostics) according to the manufacturer's directions. The sequences of primers are listed in Table S3. Relative quantification was conducted by using the comparative cycle threshold (Ct) method.

Immunocytochemistry

After fixation with 2% paraformaldehyde and blocking in 10% goat serum, the cells were stained with anti-EpCAM (Cell Signaling Technology) and anti-phospho-p38 MAPK (Cell Signaling Technology) antibodies. Subsequently, the cells were incubated with Alexa-488–conjugated goat anti-mouse immuno-

globulin G (IgG) (Molecular Probes) and Alexa-555–conjugated goat anti-rabbit IgG (Molecular Probes). The cells were coverslipped using a mounting medium containing 4′, 6-diamidino-2-phenylindole dihydrochloride (DAPI) (Vector Laboratories, Burlingame, CA). For detection of apoptosis, the cells were also stained with an anti-active caspase-3 (CASP3) antibody (Chemicon, Temecula, CA), followed by incubation with Alexa-555 conjugated goat anti-rabbit IgG (Molecular Probes).

Microarray analysis

Cy3-labeled complementary RNA was hybridized to a SurePrint G3 Human GE 8×60 K microarray (Agilent Technologies, Santa Clara, CA). Array images were scanned using a DNA Microarray Scanner (Agilent) and analyzed using Feature Extraction version 10.27.1.1. (Agilent). Normalization was performed using GeneSpring GX11.5.1 (Agilent). The expression value (Signal) for each probe set was calculated using GeneSpring GX 12.0 (Agilent). Data were obtained for triplicate samples from three independent experiments. The data were subjected to normalization using GeneSpring normalization algorithms (Agilent). Only gene expression levels with statistical significance ($p<0.05$) were recorded as being "detected" above background levels, and genes with expression levels below this statistical threshold were considered "absent." To identify differentially expressed genes in EpCAM$^+$ cells, we selected probe sets that exhibited gene expression changes with statistical significance as follows: (i) genes exhibiting a change greater than 1.5-fold ($p<0.05$), (ii) genes exhibiting a change from 1.0 to 1.5-fold ($p<0.01$), and (iii) switch-on type (upregulated from the "absent" to "present" level) and switch-off type genes (downregulated from the "present" to "absent" level) exhibiting a change greater than 4.0-fold ($p<0.01$). Moreover, functional analyses were performed using Ingenuity Pathway Analysis (IPA) version 12402621 (Ingenuity Systems). To identify gene signatures after DSF or 5-FU treatment, gene set enrichment analysis (GSEA) was also conducted [33]. The raw data are available at http://www.ncbi.nlm.nih.gov/geo/(accession number; GSE 42318).

Statistical analysis

Data are presented as the mean ± SEM. Statistical differences between 2 groups were analyzed using the Mann-Whitney U test. P values less than 0.05 were considered significant.

Supporting Information

Figure S1 *In vitro* assays of HCC cells treated with DSF. (A) Dose-dependent and time-dependent inhibition of proliferation in HCC cells treated with DSF. *Statistically significant ($p<0.05$). (B) Detection of apoptotic cell death by immunostaining for active CASP3. Nuclear DAPI staining is shown in the insets. Scale bar = 100 μm. (C) Quantification of the percentage of apoptotic cells. *Statistically significant ($p<0.05$).
(TIF)

Figure S2 In vitro assay for *ALDH2*-knockdown and double knockdown of *ALDH1* and *ALDH2*. (A) Cells transduced with the indicated lentiviruses were subjected to Western blotting using anti-*ALDH2* and anti-tubulin (loading control) antibodies. (B) Cell proliferation in *ALDH2*-knockdown HCC cells was monitored by counting cell numbers. (C) Number of primary spheres generated from 1,000 cells at day 14 of culture. (D) Cells co-transduced with the indicated lentiviruses were subjected to Western blotting using anti-*ALDH1* antibody, anti-*ALDH2* and anti-tubulin (loading control) antibodies. (E) Bright-field (upper panels) images of non-adherent spheres at day 14 of culture. Scale bar = 100 μm. EGFP and RFP expression in double-knockdown spheres are shown in the insets. (F) Number of primary spheres generated from 1,000 cells at day 14 of culture.
(TIF)

Figure S3 Flow cytometric analyses of HCC cells treated with 5-FU. Flow cytometric profiles in cells treated with 5-FU (10μg/ml) for 48 hours. The percentages of positive fractions for the indicated markers are shown as the mean values for three independent analyses.
(TIF)

Figure S4 In vitro assay of sorted EpCAM$^-$ cells treated with DSF. (A) Non-adherent sphere formation assay on EpCAM$^-$ cells at day 14 of culture. Bright-field images are shown. Scale bar = 200 μm. (B) Number of large spheres generated from 1,000 HCC cells treated with DSF. *Statistically significant ($p<0.05$). (C) Fluorescence images of EpCAM$^-$ HCC cells. The expression of p-p38 (red) was merged with nuclear DAPI staining (blue). Scale bar = 100 μm.
(TIF)

Figure S5 In vitro assay of sorted EpCAM$^+$ cells co-treated with DSF and a p38-specific inhibitor (SB203580). (A) Cell proliferation at 96 hours in culture. *Statistically significant ($p<0.05$). (B) Quantification of apoptotic cells based on the results of immunostaining for CASP3. *Statistically significant ($p<0.05$).
(TIF)

Figure S6 Gene expression profiles of EpCAM$^+$ cells treated with DSF or 5-FU. (A) Log2-fold heat map of genes involved in cell cycle in EpCAM$^+$ cells treated with DSF. (B) Quantitative RT-PCR analyses of cell cycle-related genes. *Statistically significant ($p<0.05$). (C) Gene set enrichment analysis (GSEA) of the proteasome pathway in EpCAM$^+$ cells treated with DSF or 5-FU. Both the normalized enrichment score (NES) and false discovery rate (FDR) are shown in each enrichment plot. (D) Log2-fold heat map of genes involved in the ROS scavenger pathway in EpCAM$^+$ cells treated with DSF or 5-FU.
(TIF)

Figure S7 Regulatory machinery of *GPC3* expression and loss-of-function assay of GPC3 in tumor-initiating HCC cells. (A) Quantitative RT-PCR analyses of *GPC3* expression in EpCAM$^+$ HCC cells co-treated with DSF and NAC or SB203580. *Statistically significant ($p<0.05$). (B) Quantitative RT-PCR analyses of *GPC3* expression in EpCAM$^+$ HCC cells treated with MG132. (C) Cell proliferation in *GPC3*-knockdown HCC cells at 96 hours in culture. *Statistically significant ($p<0.05$). (D) Quantification of apoptosis in cells transduced with indicated the lentiviruses based on the results of immunostaining for CASP3. *Statistically significant ($p<0.05$). (E) H&E staining and immunocytochemical analysis of EpCAM and AFP in spheres derived from EpCAM$^+$ cells. Scale bar = 20 μm. (F) Quantification of the percentage of EpCAM$^+$ or AFP$^+$ cells. *Statistically significant ($p<0.05$).
(TIF)

Figure S8 Gain-of-function assay of GPC3 in Huh1 EpCAM$^+$ cells. (A) Cells transduced with the indicated retroviruses were subjected to Western blotting using anti-GPC3 and anti-tubulin (loading control) antibodies. (B) Proliferation of Huh1 EpCAM$^+$ cells at 96 hours in culture. The percentages of cells are shown. *Statistically significant ($p<0.05$). (C) Bright–field images of Huh1 EpCAM$^+$ cells in non-adherent sphere formation at day 14 of culture. Scale bar = 100 μm. (D) Number of large spheres derived from 1,000 EpCAM$^+$ cells on day 14 of culture. *Statistically

significant ($p<0.05$). (E) Number of secondary spheres 14 days after replating. *Statistically significant ($p<0.05$).
(TIF)

Table S1 Top five ontology terms with molecular and cellular function of upregulated genes after DSF or 5-FU treatment.
(DOC)

Table S2 Top five ontology terms with molecular and cellular function of downregulated genes after DSF or 5-FU treatment.
(DOC)

Table S3 Primer sequences used for real-time RT-PCR.
(DOC)

References

1. Jordan CT, Guzman ML, Noble M (2006) Cancer stem cells. N Engl J Med 355: 1253–1261.
2. Visvader JE, Lindeman GJ (2012) Cancer stem cells: current status and evolving complexities. Cell Stem Cell 10: 717–728.
3. Ji J, Wang XW (2012) Clinical implications of cancer stem cell biology in hepatocellular carcinoma. Semin Oncol 39: 461–472.
4. Rountree CB, Mishra L, Willenbring H (2012) Stem cells in liver disease and cancer: Recent advances on the path to new therapies. Hepatology 55: 298–306.
5. Chen D, Cui QC, Yang H, Dou QP (2006) Disulfiram, a clinically used anti-alcoholism drug and copper-binding agent, induces apoptotic cell death in breast cancer cultures and xenografts via inhibition of the proteasome activity. Cancer Res 66: 10425–10433.
6. Yip NC, Fombon IS, Liu P, Brown S, Kannappan V, et al. (2011) Disulfiram modulated ROS-MAPK and NFκB pathways and targeted breast cancer cells with cancer stem cell-like properties. Br J Cancer 104: 1564–1574.
7. Liu P, Brown S, Goktug T, Channathodiyil P, Kannappan V, et al. (2012) Cytotoxic effect of disulfiram/copper on human glioblastoma cell lines and ALDH-positive cancer-stem-like cells. Br J Cancer 107: 1488–1497.
8. Cen D, Gonzalez RI, Buckmeier JA, Kahlon RS, Tohidian NB, et al. (2002) Disulfiram induces apoptosis in human melanoma cells: a redox-related process. Mol Cancer Ther 1: 197–204.
9. Wang W, McLeod HL, Cassidy J (2003) Disulfiram-mediated inhibition of NF-kappaB activity enhances cytotoxicity of 5-fluorouracil in human colorectal cancer cell lines. Int J Cancer 104: 504–11.
10. Zhang H, Chen D, Ringler J, Chen W, Cui QC, et al. (2010) Disulfiram treatment facilitates phosphoinositide 3-kinase inhibition in human breast cancer cells in vitro and in vivo. Cancer Res 70: 3996–4004.
11. Moreb JS, Baker HV, Chang LJ, Amaya M, Lopez MC, et al. (2008) ALDH isozymes downregulation affects cell growth, cell motility and gene expression in lung cancer cells. Mol Cancer 7: 87.
12. Johansson B (1992) A review of the pharmacokinetics and pharmacodynamics of disulfiram and its metabolites. Acta Psychiatr Scand Suppl 369: 15–26.
13. Suzuki E, Chiba T, Zen Y, Miyagi S, Tada M, et al. (2012) Aldehyde dehydrogenase 1 is associated with recurrence-free survival but not stem cell-like properties in hepatocellular carcinoma. Hepatol Res 42: 1100–1111.
14. Ito K, Hirao A, Arai F, Matsuoka S, Takubo K, et al. (2004) Regulation of oxidative stress by ATM is required for self-renewal of hematopoietic stem cells. Nature 431: 997–1002.
15. Diehn M, Cho RW, Lobo NA, Kalisky T, Dorie MJ, et al. (2009) Association of reactive oxygen species levels and radioresistance in cancer stem cells. Nature 458: 780–783.
16. Yamashita T, Forgues M, Wang W, Kim JW, Ye Q, et al. (2008) EpCAM and alpha-fetoprotein expression defines novel prognostic subtypes of hepatocellular carcinoma. Cancer Res 2008;68:1451–1461.
17. Schaefer CF, Anthony K, Krupa S, Buchoff J, Day M, et al. (2009) PID: the Pathway Interaction Database. Nucleic Acids Res 37(Database issue): D674–679.
18. Science Signaling Web Site. Available: http://stke.sciencemag.org/cgi/cm/stkecm;CMP_10958 Accessed 2012 January 3.
19. Wong DJ, Nuyten DS, Regev A, Lin M, Adler AS, et al. (2008) Revealing targeted therapy for human cancer by gene module maps. Cancer Res 68: 369–378.
20. Midorikawa Y, Ishikawa S, Iwanari H, Imamura T, Sakamoto H, et al. (2003) Glypican-3, overexpressed in hepatocellular carcinoma, modulates FGF2 and BMP-7 signaling. Int J Cancer 103: 455–465.
21. Liu S, Li Y, Chen W, Zheng P, Liu T, et al. (2012) Silencing glypican-3 expression induces apoptosis in human hepatocellular carcinoma cells. Biochem Biophys Res Commun 419: 656–661.
22. Marchitti SA, Brocker C, Stagos D, Vasiliou V (2008) Non-P450 aldehyde oxidizing enzymes: the aldehyde dehydrogenase superfamily. Expert Opin Drug Metab Toxicol 4: 697–720.
23. Dollé L, Best J, Empsen C, Mei J, Van Rossen E, et al. (2012) Successful isolation of liver progenitor cells by aldehyde dehydrogenase activity in naïve mice. Hepatology 55: 540–552.
24. Ginestier C, Hur MH, Charafe-Jauffret E, Monville F, Dutcher J, et al. (2007) ALDH1 is a marker of normal and malignant human mammary stem cells and a predictor of poor clinical outcome. Cell Stem Cell 1: 555–567.
25. Tothova Z, Kollipara R, Huntly BJ, Lee BH, Castrillon DH, et al. (2007) FoxOs are critical mediators of hematopoietic stem cell resistance to physiologic oxidative stress. 128: 325–339.
26. Ito K, Hirao A, Arai F, Takubo K, Matsuoka S, et al. (2006) Reactive oxygen species act through p38 MAPK to limit the lifespan of hematopoietic stem cells. Nat Med 12: 446–451.
27. Ishimoto T, Nagano O, Yae T, Tamada M, Motohara T, et al. (2011) CD44 variant regulates redox status in cancer cells by stabilizing the xCT subunit of system xc- and thereby promotes tumor growth. Cancer Cell 19: 387–400.
28. Sawada Y, Yoshikawa T, Nobuoka D, Shirakawa H, Kuronuma T, et al. (2012) Phase I trial of a glypican-3-derived peptide vaccine for advanced hepatocellular carcinoma: immunologic evidence and potential for improving overall survival. Clin Cancer Res 18: 3686–3696.
29. Grozdanov PN, Yovchev MI, Dabeva MD (2006) The oncofetal protein glypican-3 is a novel marker of hepatic progenitor/oval cells. Lab Invest 86: 1272–1284.
30. Gilbertson RJ, Rich JN (2007) Making a tumour's bed: glioblastoma stem cells and the vascular niche. Nat Rev Cancer 7: 733–736.
31. Calabrese C, Poppleton H, Kocak M, Hogg TL, Fuller C, et al. (2007) A perivascular niche for brain tumor stem cells. Cancer Cell 11: 69–82.
32. Iwama A, Oguro H, Negishi M, Kato Y, Morita Y, et al. (2004) Enhanced self-renewal of hematopoietic stem cells mediated by the polycomb gene product Bmi-1. Immunity 21: 843–851.
33. Subramanian A, Tamayo P, Mootha VK, Mukherjee S, Ebert BL, et al. (2005) Gene set enrichment analysis: a knowledge-based approach for interpreting genome-wide expression profiles. Proc Natl Acad Sci U S A 102: 15545–15550.

Acknowledgments

The authors thank Dr. Fumihiko Kanai (Medical Corporation Eikenkai) and Dr. Motohisa Tada (Chiba University) for valuable discussions.

Author Contributions

Conceived and designed the experiments: TC ES KY YZ. Performed the experiments: TC ES KY YZ MO SM AS S. Koide. Analyzed the data: TC ES KY YZ TM SO YO AT. Contributed reagents/materials/analysis tools: TN TH TY S. Kaneko MM AI OY. Wrote the paper: TC AI.